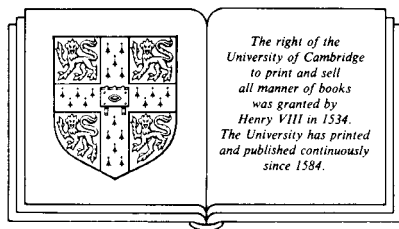


# VORTEX ELEMENT METHODS FOR FLUID DYNAMIC ANALYSIS OF ENGINEERING SYSTEMS

R. I. LEWIS

Professor of Fluid Mechanics and Thermodynamics  
University of Newcastle upon Tyne



CAMBRIDGE UNIVERSITY PRESS  
Cambridge  
New York Port Chester  
Melbourne Sydney

Published by the Press Syndicate of the University of Cambridge  
The Pitt Building, Trumpington Street, Cambridge CB2 1RP  
40 West 20th Street, New York, NY 10011, USA  
10 Stamford Road, Oakleigh, Melbourne 3166, Australia

© Cambridge University Press 1991

First published 1991

British Library cataloguing in publication data

Lewis, R. I. (Reginald Ivan) 1930–

Vortex element methods for fluid dynamic analysis of  
engineering systems.

1. Fluids. Applied dynamics. Mathematics. Numerical methods

I. Title

620.106401511

Library of Congress cataloguing in publication data available

ISBN 0 521 36010 2 hardback

Transferred to digital printing 2003

# Contents

<i>Preface</i>	xvii
<i>Acknowledgements</i>	xxi

## **Part 1 The surface vorticity method for inviscid ideal fluid flow**

### **Chapter 1 The basis of surface singularity modelling**

1.1 Introduction	3
1.2 The source panel or Douglas–Neumann method	5
1.3 The surface vorticity or Martensen method	8
1.4 Physical significance of the surface vorticity model	10
1.5 Vorticity convection and production in a shear layer	14
1.6 Surface vorticity model for plane two-dimensional flow	17
1.6.1 Self-induced velocity of a surface vorticity element due to curvature	22
1.6.2 Computational scheme for surface vorticity analysis	25
1.7 Comparison of surface vorticity analysis with Douglas–Neumann scheme	27
1.8 Calculation of streamlines and velocities within the flow field	32
1.9 Flows with symmetry about the $x$ axis	35
1.10 Generalised equations for surface vorticity modelling in curvilinear coordinates	39

### **Chapter 2 Lifting bodies, two-dimensional aerofoils and cascades**

2.1 Introduction	44
2.2 Circular cylinder with bound circulation – Flettner rotor	45
2.3 Flow past a thin ellipse	49
2.3.1 Reconsideration of non-lifting ellipse	50

## *Contents*

2.3.2	Use of sub-elements	55
2.3.3	Back diagonal correction	56
2.4	Thin ellipse as a lifting aerofoil	59
2.4.1	Kutta condition, method 1 – prescribed bound circulation $\Gamma$	59
2.4.2	Kutta condition, method 2 – trailing edge unloading	60
2.4.3	Method 3 – Wilkinson’s Kutta condition	63
2.5	Aerofoils	66
2.5.1	Unit solutions	67
2.5.2	Specification of aerofoil geometry	68
2.5.3	Comparison with Joukowski aerofoils	69
2.6	Turbomachine linear cascades	75
2.6.1	Cascade coupling coefficients	75
2.6.2	Cascade dynamics and parameters	79
2.6.3	Program Bladerow.pas and sample calculations	81
2.7	Multiple bodies and aerofoils with slots and flaps	92
2.7.1	Internal circulation correction for bodies in close proximity	94
2.7.2	Assemblies of lifting aerofoils	96
 <b>Chapter 3 Mixed-flow and radial cascades</b>		
3.1	Introduction	99
3.2	Transformation of a mixed-flow cascade into a straight cascade	102
3.2.1	Axial and radial blade rows	105
3.3	Sample calculation for an outflow radial diffuser vane cascade	108
3.3.1	Surface pressure distribution	109
3.3.2	Inlet and outlet angles	109
3.4	Rotor/stator interference in centrifugal compressors	110
3.5	Mixed-flow and radial rotor blade rows	112
3.5.1	Transformation of the ‘relative eddy’ to the straight cascade plane	114
3.5.2	Correction for irrotationality of the inner blade profile region	117
3.5.3	Influence of meridional streamline thickness (AVR)	122
3.5.4	Unit solutions for mixed-flow cascades and prediction of flow angles	124

## *Contents*

3.5.5	More precise method for removal of profile internal vorticity	126
3.6	Comparison with exact solutions for radial cascades by conformal transformation	134
3.6.1	Flow analysis of the transformation	137
3.6.2	Sample solutions	139
3.6.3	Comparisons with experimental test	141
3.7	Effects of AVR in compressor cascades	143
<b>Chapter 4 Bodies of revolution, ducts and annuli</b>		
4.1	Introduction	146
4.2	The axisymmetric surface vorticity model	147
4.2.1	Evaluation of complete elliptic integrals. Use of look-up tables	150
4.2.2	Numerical representation of the integral equation for axisymmetric flow	153
4.2.3	Self-induced velocity of a ring vorticity element	154
4.3	Flow past a body of revolution	157
4.3.1	Flow past a sphere	158
4.3.2	Flow past a body of revolution	159
4.4	Annular aerofoils or engine cowls	160
4.5	The semi-infinite vortex cylinder	167
4.6	Flow through a contraction	170
4.7	Flow through an annulus	174
4.8	Source panel solutions for plane two-dimensional and axisymmetric flows	176
4.8.1	Source panel modelling of lifting aerofoils	177
4.9	Source panel method for axisymmetric flows	183
4.9.1	Source panel method for a body of revolution	185
4.9.2	Source panel method for an annular aerofoil or engine cowl	187
<b>Chapter 5 Ducted propellers and fans</b>		
5.1	Introduction	191
5.2	The sucked-duct or pipe-flow engine intake facility	192
5.3	Free vortex ducted propeller	198
5.4	Non-free vortex ducted propeller – lifting surface theory	204

## *Contents*

5.4.1 Matching the helix angle	209
5.4.2 Propeller loading and vortex shedding	212
5.5 Vorticity production in axisymmetric meridional flows	214
5.5.1 Streamwise and smoke-ring vorticity	217
5.6. Non-free vortex actuator disc model for axial turbomachines and ducted propellers	218
5.7 Models to deal with the induced effects of distributed ring vorticity in axisymmetric meridional flows	221
5.7.1 Numerical representation of rectangular and circular ring vortex elements	221
5.7.2 Check on self-propagation of a smoke-ring vortex	224
5.7.3 Self-propagation of a sheet ring vortex element	225
5.7.4 Induced velocities close to a rectangular ring vortex	225
5.7.5 Flow of a shear layer past a body of revolution	227
<b>Chapter 6 Three-dimensional and meridional flows in turbomachines</b>	
6.1 Introduction	233
6.2 Three-dimensional flow past lifting bodies	234
6.3 Three-dimensional flow past annular aerofoils and engine cowls	240
6.3.1 Numerical scheme using circumferential series expansions	243
6.4 Sweep and dihedral in turbomachine blade rows	248
6.4.1 Swept aerofoils and cascades of infinite aspect ratio	251
6.4.2 Swept cascade of finite aspect ratio	256
6.4.3 Analysis with constant spanwise loading	259
6.4.4 Analysis with variable spanwise loading in three-dimensional flow	261
6.5 Local blade rake and lean and blade forces	264
6.5.1 Local blade forces	266
6.6 Equations of meridional flow for bladed regions	268
6.7 Axisymmetric meridional flows in mixed-flow turbomachines	271
6.7.1 Flow through an actuator disc in a cylindrical annulus	273
6.7.2 Meridional flow through a mixed-flow turbomachine	275

*Contents*

**Part 2 Free shear layers, vortex dynamics and vortex cloud analysis**

**Chapter 7 Free vorticity shear layers and inverse methods**

7.1 Introduction	281
7.2 The free-streamline model	282
7.3 Free jets	289
7.4 Inverse aerofoil design	291
7.4.1 Basis of inverse surface vorticity design method for aerofoils and cascades	292
7.4.2 Further refinements	295
7.4.3 Angular constraints on leading and trailing edge elements	297
7.4.4 Aerofoil inverse design	301
7.5 Inverse design of cascades and slotted cascades	303
7.5.1 True inverse design method for cascades	304
7.5.2 Inverse cascade design by iterative use of the direct method	306
7.6 Inverse design of axisymmetric bodies	309

**Chapter 8 Vortex dynamics in inviscid flows**

8.1 Introduction	316
8.2 Vortex convection	319
8.2.1 Convection of a vortex pair	320
8.3 Convection and stability of vortex sheets	326
8.3.1 Roll-up of a free-ended vortex sheet	327
8.3.2 Kelvin–Helmholtz instability of a vortex sheet	329
8.4 Convective interaction of free vortices with solid bodies	337
8.4.1 Potential flow past a cylinder due to a nearby vortex	339
8.4.2 Convection of a free vortex near a circle or an ellipse	347
8.4.3 Convection of vortices in very close proximity to a body	351
8.5 Simple vortex cloud modelling for two-dimensional bodies with prescribed separation points	354
8.5.1 Vorticity shedding from a sharp edge separation point	355

## *Contents*

8.5.2	Simple vortex dynamics scheme for simulation of wake development	356
8.5.3	Vorticity shedding from a smooth surfaced bluff body	358
<b>Chapter 9 Simulation of viscous diffusion in discrete vortex modelling</b>		
9.1	Introduction	364
9.2	Diffusion of a point vortex in two-dimensional flow	366
9.2.1	Random number generation	370
9.2.2	Radial distribution of vorticity $\omega(r)$	371
9.2.3	Diffusion over a series of time steps	372
9.3	Diffusion of a vortex sheet	374
9.4	Boundary layers by discrete vortex modelling	377
9.4.1	Vorticity creation and shedding (Step 2)	378
9.4.2	Viscous diffusion (Step 3)	381
9.4.3	Vortex convection (Step 5)	381
9.4.4	Vortices in close proximity (Step 6)	382
9.4.5	Calculation of velocity profile (Step 9)	384
9.4.6	Selection of element size and time step	387
9.4.7	Some considerations for high Reynolds number flows	388
<b>Chapter 10 Vortex cloud modelling by the boundary integral method</b>		
10.1	Introduction	393
10.2	Vortex cloud modelling with prescribed separation points	395
10.2.1	Introduction of reduced circulation	398
10.2.2	Time growth of the vortex core	400
10.3	Application of fixed separation point analysis to a lifting aerofoil	400
10.4	Full vortex cloud modelling by the surface vorticity boundary integral method	404
10.4.1	Potential flow analysis in the presence of a vortex cloud	407
10.4.2	Vortex shedding from body surface	409
10.4.3	Convection schemes. Method 1, strict Eulerian convection. Method 2, simplified Eulerian convection	410

## *Contents*

10.5	Calculation of surface pressure distribution and body forces	413
10.5.1	Pressure distribution – full vortex cloud model	414
10.5.2	Pressure distribution – vortex cloud modelling with fixed separation points	415
10.5.3	Pressure and force fluctuations due to numerical noise	417
10.5.4	Data reduction of unsteady pressures and forces for bluff body flows	420
10.6	Application of vortex cloud analysis to flow past a circular cylinder	422

### **Chapter 11 Further development and applications of vortex cloud modelling to lifting bodies and cascades**

11.1	Introduction	428
11.2	Flow past a lifting aerofoil by vortex cloud analysis	428
11.3	Alternative vortex cloud modelling techniques by Spalart & Leonard	434
11.3.1	NACA 0012 aerofoil in dynamic stall	437
11.4	Mixed vortex cloud and potential flow modelling	441
11.4.1	Lifting aerofoil by the hybrid potential flow/vortex cloud method	443
11.4.2	Aerofoil with airbrake spoiler by the hybrid potential flow/vortex cloud method	445
11.4.3	Aerofoils with moving spoilers	450
11.5	Application of vortex cloud modelling to turbomachinery blade rows	451
11.5.1	Vortex cloud analysis for periodic flow through linear cascades	451
11.5.2	Rotating stall in compressors	459
11.6	Flow induced acoustic resonance for a bluff body in a duct	463
11.7	Potential for future development of vortex cloud analysis	467

### **Chapter 12 Use of grid systems in vortex dynamics and meridional flows**

12.1	Introduction	469
12.2	Cell-to-cell interaction method for speeding convective calculations	470

## *Contents*

12.3	Cloud-in-cell (CIC) method	476
12.3.1	Vortex re-distribution to cell corners	477
12.3.2	Convection with grid distribution of vorticity	478
12.4	Cellular modelling of viscous boundary layers	483
12.4.1	Numerical solution for a diffusing vortex sheet	483
12.4.2	Diffusion coupling coefficient matrices	487
12.4.3	Boundary layer simulation by the cell method	489
12.4.4	The Blasius boundary layer	492
12.4.5	Similarity boundary layers	493
12.4.6	Selection of grid data for cellular boundary layer computational schemes	497

### **Appendix Computer Programs**

Program 1.1	Flow past a circular cylinder including surface velocity, comparison with exact solution.	499
Program 1.2	Flow past a circular cylinder by the Douglas-Neumann source panel method.	502
Program 1.3	Flow past an ellipse, including surface velocity comparison with exact solution and streamline pattern.	505
Program 2.1	Calculation of flow past a cylinder with bound circulation.	508
Program 2.2	Flow past an ellipse with prescribed bound circulation.	510
Program 2.3	Potential flow past an aerofoil.	512
Program 2.4	Potential flow through a turbomachine cascade.	515
Program 4.1	Calculation of complete elliptic integrals of the first and second kinds.	518
Program 4.2	Flow past a body of revolution.	521
Program 4.3	Flow past an axisymmetric cowl or duct.	524
Program 4.4	Flow through a contraction or diffuser.	526
Program 4.5	Flow past a body of revolution in a uniform stream.	530
Program 5.1	Potential flow through an engine intake sucked from downstream by a cylindrical duct and located in a uniform stream (Pipe flow test rig).	533
Program 5.2	Potential flow through a free-vortex ducted propeller in a uniform stream.	537

## *Contents*

Program 8.1	Program for experimentation with convection of vortex clouds.	540
Program 9.1	Program to generate a set of random numbers and sort them.	543
Program 9.2	Diffusion of a point vortex.	544
	<i>Bibliography</i>	547
	<i>Index</i>	560

## CHAPTER 1

# The basis of surface singularity modelling

### 1.1 Introduction

The principal aims of this book are to outline the fundamental basis of the surface vorticity boundary integral method for fluid flow analysis and to present a progressive treatment which will lead the reader directly to practical computations. Over the past two and a half decades the surface vorticity method has been developed and applied as a predictive tool to a wide range of engineering problems, many of which will be covered by the book. Sample solutions will be given throughout, sometimes related to Pascal computer programs which have been collated for a selection of problems in the Appendix. The main aims of this introductory chapter are to lay down the fundamental basis of both source and vorticity surface panel methods, to explain the fluid dynamic significance of the surface vorticity model and to introduce a few initial applications to potential flow problems.

As numerical techniques, surface singularity methods were not without progenitors but grew quite naturally from the very fertile field of earlier linearised aerofoil theories. Such methods, originally contrived for hand calculations, traditionally used internal source distributions to model profile thickness and vortex distributions to model aerodynamic loading, a quite natural approach consistent with the well known properties of source and vortex singularities. On the other hand it can be shown that the potential flow past a body placed in a uniform stream can be modelled equally well by replacing the body surface with either a source or a vortex sheet of appropriate strength, Fig. 1.1. Integral equations can then be written expressing the Neumann boundary condition of zero normal surface velocity for the source model or the Dirichlet condition of zero parallel surface velocity for the vorticity model. Whichever type of singularity is chosen the final outcome is the same, namely a prediction of the potential flow velocity close to the body profile. The numerical strategy is also fairly similar as we shall see from

*The basis of surface singularity modelling*

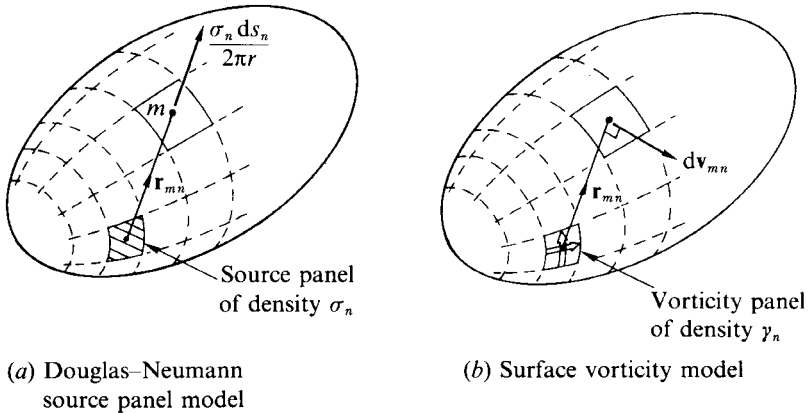


Fig. 1.1. Surface source and vorticity panel models for three-dimensional potential flow.

Sections 1.6 and 1.7. Lifting bodies form an important exception to this remark, since lift forces normal to a uniform stream cannot be simulated by sources alone but require also the introduction of vorticity distributions, a matter which will be taken up in Chapter 2. On the other hand the surface vorticity model is capable of handling potential flows for any situation including lifting bodies. We shall begin in Sections 1.2 and 1.3 with a presentation of these basic surface singularity models and their associated integral equations.

Surface vorticity modelling offers the additional advantage over source panels that it actually represents a direct simulation of an ideal fluid flow. In all real flows a boundary viscous shear layer exists adjacent to the body surface. Inviscid potential flow is akin to the case of the flow of a real fluid at infinite Reynolds number for which the boundary layer is of infinitesimal thickness. In this situation the boundary layer vorticity is squashed into an infinitely thin vorticity sheet across which the velocity parallel to the surface changes discontinuously from zero in contact with the wall to the potential flow value just outside the vorticity sheet. Thus surface vorticity modelling is the most natural of all boundary integral techniques. Further discussion of its physical significance will be given in Section 1.4. Part I of this book is concerned with such ideal flows for a range of applications especially in the fields of aerodynamics and rotodynamic machines including also some situations involving rotational main stream flow. In the early sections of Part II further consideration will be given to the physical sig-

## Introduction

nificance of the surface vorticity model including its extension to the simulation of real boundary layer flows and the establishment of wake eddies behind bluff bodies.

Surface source modelling by contrast is capable of no direct physical interpretation but is purely a vehicle, albeit a powerful one, for analysing three-dimensional potential flows. Historically it predated the surface vorticity method by half a decade or so as an emerging practical tool for numerical analysis at a time of intense pressure for the creation of flexible computational procedures for design use in the aeronautical field. To some extent surface vorticity methods were thus upstaged and have consequently received but a small fraction of the attention paid to the surface source panel technique. This book is aimed at redressing the balance. Although most of the text will in consequence be concerned with surface vorticity theory and applications, we will devote some of chapter 1 to consideration in parallel of both source and vorticity panel methods. Following the introductory Sections 1.2 to 1.5 on fundamentals we will move on quickly to numerical models for plane two-dimensional flows in Sections 1.6 and 1.7, leading to comparisons between the source and vorticity schemes for flow past a circle and an ellipse. One or two other plane two-dimensional problems will then be dealt with in Section 1.9 involving bodies with sharp corners and simplifications for symmetrical bodies. The chapter is concluded with a summary of the surface vorticity equations expressed in curvilinear coordinates.

### 1.2 The source panel or Douglas–Neumann method

Many of today's established numerical methods for engineering design and analysis find their origins in classical mathematics predating the age of the digital computer. Surface singularity methods are no exception. For example in 1929 Kellogg wrote a comprehensive book dealing with potential theory by the use of integral equations, including the treatment of volume and surface singularities. Such works tended to concentrate upon solutions to incompressible inviscid flows, expressed for example by Laplace's equation for the velocity potential  $\phi$

$$\nabla^2 \phi = \frac{\partial^2 \phi}{\partial x^2} + \frac{\partial^2 \phi}{\partial y^2} + \frac{\partial^2 \phi}{\partial z^2} = 0 \quad (1.1)$$

### *The basis of surface singularity modelling*

where  $(x, y, z)$  are Cartesian coordinates. A well known elementary solution to this equation is given by  $\phi = 1/r$  where  $r$  is the radial distance between  $(x_n, y_n, z_n)$  and some other point of fluid action  $(x_m, y_m, z_m)$ . The physical interpretation of this solution is that of flow from a point source in three-dimensional space. Thus, the velocity potential at  $m$  due to a point source of unit strength at  $n$  (where point source strength is defined here as the volume of fluid emitted in unit time) is given by

$$\phi = -\frac{1}{4\pi r_{mn}} \quad (1.2)$$

where

$$r_{mn} = \{(x_m - x_n)^2 + (y_m - y_n)^2 + (z_m - z_n)^2\}^{1/2} \quad (1.3)$$

As shown by Kellog (1929) and elaborated by A. M. O. Smith (1962), the flow past a body immersed in a uniform stream  $W_\infty$  may then be expressed by the following integral equation,

$$\frac{1}{2}\sigma_m - \frac{1}{4\pi} \iint_S \frac{\partial}{\partial n} \left( \frac{1}{r_{mn}} \right) \sigma_n dS_n + \mathbf{i}_m \cdot \mathbf{W}_\infty = 0 \quad (1.4)$$

where  $\mathbf{i}_m$  is a unit vector normal to the body surface  $S$ , and  $\sigma_n$  is the source density per unit area. This equation represents the earliest form of surface singularity model in which the body surface is replaced by a surface source distribution  $\sigma_n$ , Fig. 1.1(a). Equation (1.4) then states the Neumann boundary condition that for all points  $m$  on the body the velocity normal to the surface is zero. If this equation is satisfied then the body surface becomes a stream surface of the flow. For computation we may complete the normal derivative inside the Kernel resulting in

$$\frac{1}{2}\sigma_m + \frac{1}{4\pi} \iint_S \frac{\sigma_n}{r_{mn}^3} \mathbf{r}_{mn} \cdot \mathbf{i}_m dS_n + \mathbf{i}_m \cdot \mathbf{W}_\infty = 0 \quad (1.5)$$

This equation states that the sum of three velocity components normal to the surface at point  $m$ , when combined, comes to zero. The last term is the component of the uniform stream resolved along the surface normal  $\mathbf{i}_m$ . The second term accounts for the influence of all surface source elements  $\sigma_n dS_n$ . Here we note that the actual velocity at  $m$  due to one such element is given by

$$dv_{mn} = \frac{\sigma_n dS_n}{4\pi r_{mn}^2} \quad (1.6)$$

### *The source panel or Douglas–Neumann method*

and has the vector direction of  $\mathbf{r}_{mn}$ , which can be represented by the unit vector  $\mathbf{r}_{mn}/r_{mn}$ . Since the integral is taken actually on the surface  $S$ , we must introduce also the first term of (1.5),  $\frac{1}{2}\sigma_m$ , which represents the velocity discontinuity stepping onto the outside of the source sheet.

The numerical strategy of the panel method involves the representation of the body surface by a finite distribution of source panels defined geometrically by a suitable grid, Fig. 1.1(a). One control point  $m$  is chosen for each source panel for application of the Neumann boundary condition through (1.5). The surface integral then becomes a summation for all panels, resulting in a set of  $M$  linear equations for  $M$  unknown values of  $\sigma_m$ . Solution is straightforward usually and yields the necessary surface source strength to ensure that the flow remains parallel to the body surface. Following on from this the local potential flow velocity parallel to the surface can be evaluated directly by means of a second integral equation of the form,

$$\mathbf{v}_m = \mathbf{i}_m X \left\{ \frac{1}{4\pi} \iint_S \frac{\sigma_n}{r_{mn}^3} \mathbf{r}_{mn} X \mathbf{i}_m dS_n + \mathbf{W}_\infty X \mathbf{i}_m \right\} \quad (1.7)$$

This has been expressed in vector form, reminding us that for three-dimensional bodies the surface potential flow is of course two-dimensional. Reduction to Cartesian or other coordinate systems is necessary for numerical computations but is soon accomplished. Later, in Section 1.7, we will illustrate this by a simple numerical example, but for the present our aim is to draw out some of the fundamental equations and models of surface singularity methods. In the case of the source panel method, which is actually not to be the main substance of this book, it remains only to point out that two integral equations must be solved, one indirect and the other direct, using the source ‘singularity’ distribution  $\sigma_m$  as an intermediate parameter for reaching the solution. Unlike the use of surface vorticity, source panels provide no ready physical interpretation or special advantage as a physical model except in very special cases such as surface transpiration or change in fluid volume due to evaporation or condensation at a surface. Nevertheless, as a computational method for potential flows the source panel method has been widely used with great success since about 1953, notably in the field of aeronautics. The literature is extensive and mention will be made here only of representative early work by A. M. O. Smith (1962), A. M. O. Smith & Hess (1966), A. M. O. Smith & Pierce

### *The basis of surface singularity modelling*

(1958) and Hess (1962) covering basic theory with a range of applications. A more recent survey of models and formulations was also given by Hunt (1978). Discussions of the relationships between volume surface and line distributions of vorticity, sources and doublets have been given by Semple (1977), Hunt (1978) and R. Rohatynski (1986).

### **1.3 The surface vorticity or Martensen method**

Although no doubt early theorems related to surface vorticity distributions, such as those of Kellogg previously referred to, could be located in older texts, the seed corn publication in this field was undoubtedly that of Martensen (1959). Martensen not only laid out the basis of a powerful new computational technique, but he also extended his new boundary integral theory to deal with turbo-machine cascades, a subject which we will deal with in some detail in Chapters 2 and 3. However, Jacob & Riegels (1963) would seem to have been the first contributors of a practical working scheme designed for digital computers, taking 15 minutes to execute on a IBM 650 computer for analysis of an aerofoil with 36 surface vorticity elements; no mean achievement at that time. Numerical modelling often offers great scope for ingenuity and inventiveness and several good ideas put forward by Jacob and Riegels have stood the test of time. However there were many problems to be identified and solved before the method could progress to acceptability as a reliable engineering predictive tool. D. H. Wilkinson pioneered many of these problems of modelling and practical methodology, publishing a most significant paper in 1967 which formed an important foundation stone for computer applications. He also extended his work to mixed-flow cascades, Wilkinson (1969), another very important and far reaching contribution. In parallel with this Nyiri (1964), (1970) independently produced an extension of Martensen's method to mixed-flow pump cascades, later updated as a practical numerical scheme, Nyiri & Baranyi (1983). There are of course many other important publications covering a range of applications. These will not be reviewed here but referred to in relevant parts of the text.

The surface vorticity model is illustrated in Fig. 1.1(b) for a three-dimensional body. In this scheme the body surface is covered with a finite number of surface vorticity panels initially of unknown

*The surface vorticity or Martensen method*

strength. Following a similar procedure to the source panel method, one control point  $m$  is chosen for each panel for application of the surface flow boundary condition, taking account of the influence of all other surface vorticity panels and of the mainstream flow. In this case on the other hand, it is appropriate to adopt the boundary condition of zero velocity on, and parallel to the body surface†, (we shall consider why in more detail later in Section 1.4). The actual velocity induced at  $m$  by a small line vortex element at  $n$  of strength  $\Gamma_n$  per unit length\* and of length  $dl_n$  is given by the Biot–Savart law, namely, with reference to Fig. 1.2,

$$d\mathbf{v}_{mn} = \frac{\Gamma_n dl_n \mathbf{i}_m \times \mathbf{r}_{mn}}{4\pi r_{mn}^3} \quad (1.8)$$

By taking the cross product of  $d\mathbf{v}_{mn}$  with the unit vector  $\mathbf{i}_m$  normal to the surface at  $m$  twice, we obtain the velocity parallel to the surface at  $m$  induced by the line vortex element. Thus

$$\begin{aligned} d\mathbf{v}_{smn} &= \mathbf{i}_m \times (d\mathbf{v}_{mn} \times \mathbf{i}_m) \\ &= \frac{\mathbf{i}_m \times ((\Gamma_n \mathbf{i}_m \times \mathbf{r}_{mn}) \times \mathbf{i}_m) dl_n}{4\pi r_{mn}^3} \end{aligned} \quad (1.9)$$

In reality the surface is to be covered not with concentrated line vortices but with an area density of distributed sheet vorticity which

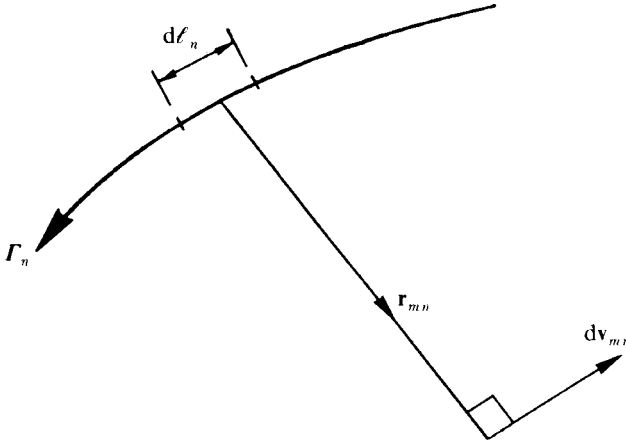


Fig. 1.2. Velocity induced by a line vortex element.

† Since we are addressing the Dirichlet problem for  $\mathbf{q}$  this will be termed the Dirichlet boundary condition throughout this book.

\* Throughout this book vortex strength is defined as positive according to the right hand corkscrew rule.

### *The basis of surface singularity modelling*

we will denote here by the symbol  $\gamma_m$ . Making use of (1.9) the Dirichlet boundary condition of zero velocity on (and parallel to) the body surface at  $m$  may then be expressed

$$-\frac{1}{2}\gamma_m + \frac{1}{4\pi} \iint_S \frac{\mathbf{i}_m X((\gamma_n X \mathbf{r}_{mn}) X \mathbf{i}_m) dS}{r_{mn}^3} + \mathbf{i}_m X(\mathbf{W}_\infty X \mathbf{i}_m) = 0 \quad (1.10)$$

The last term is the component of the mainstream velocity  $\mathbf{W}_\infty$  resolved parallel to the body surface. The first term is the velocity discontinuity experienced if we move from the centre of the vorticity sheet onto the body surface beneath.

As it stands this integral equation, like that for the source panel method (1.5), is of little practical use and is recorded here only in view of its importance as a general statement of the problem. We will later on in Section 1.10 express it in curvilinear coordinates which are of much more value for setting up computational schemes in various coordinate systems. At this point however it will be much more helpful to move on to a simple physical interpretation of the surface vorticity method followed by practical application to a numerical scheme for solving a simple problem.

## **1.4 Physical significance of the surface vorticity model**

In all real flows a boundary shear layer develops adjacent to the surface of a body, Fig. 1.3(a). Sufficient vorticity is present in this layer to reduce the fluid velocity from  $v_s$  just outside the shear layer to a value of zero on the body surface. The action of viscosity is to cause the vorticity in this shear layer to diffuse normal to the surface, resulting in the familiar viscous boundary layer. The vorticity itself however is the product of the dynamic behaviour of the outer flow and we will show later that the rate of vorticity production adjacent to the surface is directly related to the pressure gradient. Traditionally a real flow is usually regarded as comprising a largely irrotational inviscid outer flow in the bulk of the domain, separated from the body surface by a thin but highly active viscous shear layer. These regimes are of course frequently treated separately for analytical expediency, with suitable matching conditions at the outer edge  $a-b$  of the boundary layer. In reality, as we have just pointed out, vorticity creation is largely attributable to the outer flow, a fact which is underlined if we consider in particular the special case of infinite Reynolds number, or inviscid potential flow.

*Physical significance of the surface vorticity model*

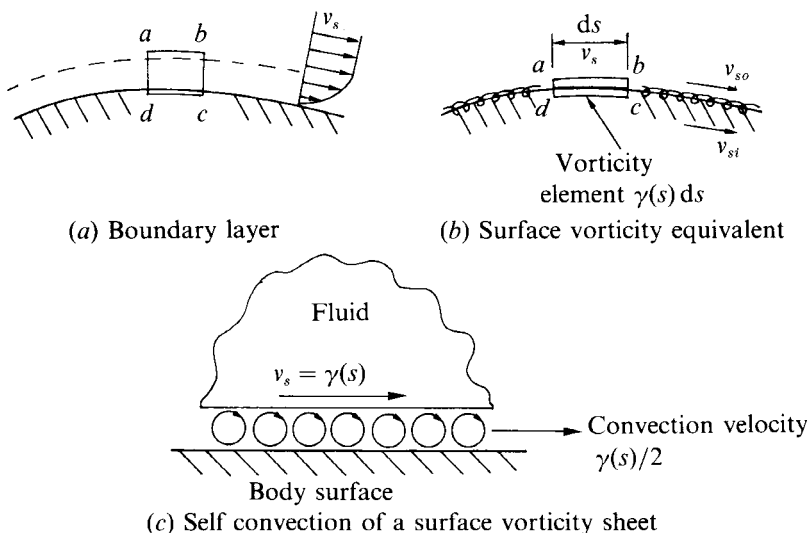


Fig. 1.3. Boundary layer and surface vorticity equivalent in potential flow.

Suppose that we were able gradually to reduce the fluid viscosity to zero in a real fluid flow. In the limit, due to progressive reduction of viscous diffusion, the boundary layer would approach infinitesimal thickness. As the viscosity approached zero and the Reynolds number approached infinity, the body surface would be covered with an infinitely thin vorticity sheet  $\gamma(s)$ , Fig. 1.3(b), across which the fluid velocity would change discontinuously from zero beneath the sheet on the body surface to  $v_s$  parallel to the surface just above the sheet. In the case of a real flow with extremely high Reynolds number, we are aware that the boundary layer may separate spontaneously with rising static pressure in the direction of the mainstream flow. Furthermore the boundary layer will normally become turbulent at very high Reynolds numbers. Both phenomena are connected with the interrelationship between the viscous diffusion and convection processes in the boundary layer which the Reynolds number symbolises. Leaving aside these additional features of a real flow connected with instabilities of the shear layer itself, we see that inviscid potential flows can be thought of as a special type of infinite Reynolds number flow. An irrotational potential flow thus comprises a surface vorticity sheet covering the body surface, separating the irrotational flow of the outer domain from a motionless flow in the inner domain. In this sense the surface

### *The basis of surface singularity modelling*

vorticity model is precisely true to the physical reality of a real infinite Reynolds number (but fully attached) flow and is therefore the most natural of all numerical methods for potential flow analysis. Furthermore, as we shall see in Chapters 9–11, it is also possible to introduce models to simulate viscous diffusion, so that we may relax the present constraint of infinite Reynolds number. The surface vorticity method, unlike the source panel method, thus offers special attractions as a route towards the simulation of real fluid flows because the model truly reflects the physical reality, Lewis & Porthouse (1983a).

To decide upon an appropriate boundary condition (which we have already asserted to be the Dirichlet condition) let us consider the flow induced by such a surface vorticity sheet in closer detail, Fig. 1.3. First let us define the contour  $abcd$  surrounding a small vorticity element  $\gamma(s) ds$  where  $ab$  and  $dc$  are parallel to the streamlines, while  $da$  and  $cb$  are normal to them. Now  $\gamma(s)$  is defined as the vorticity strength per unit length at point  $s$ . The circulation around  $abcd$ , defined clockwise–positive, may be equated to the total amount of vorticity enclosed by the contour, that is

$$(v_{so} - v_{si}) ds = \gamma(s) ds$$

where  $v_{so}$  and  $v_{si}$  are the fluid velocities just outside and inside the sheet, which must be parallel to the surface. Our boundary condition of zero velocity on the body surface is thus satisfied if we specify

$$v_{si} = 0 \tag{1.11}$$

whereupon

$$v_{so} = v_s = \gamma(s) \tag{1.12}$$

The neatness of Martensen's method lies in these two equations. Equation (1.11) is the basis of Martensen's boundary integral equation as summarised previously by (1.10). The solution of this equation yields the surface vorticity distribution of the potential flow. The second equation (1.12) then tells us that the potential flow velocity close to the body surface  $v_s$  is now immediately known, being exactly equal to the surface vorticity  $\gamma(s)$ . The surface vorticity method, in addition to its direct simulation of physical reality, thus offers the additional attraction compared with the source panel method that no second integral equation is required to derive  $v_s$  from the surface singularity distribution.

*Physical significance of the surface vorticity model*

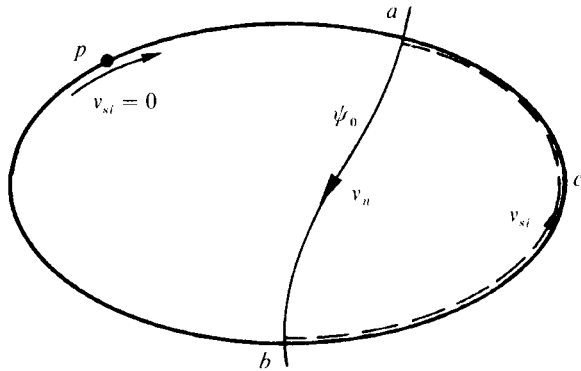


Fig. 1.4. Check for leakage flow with the Dirichlet boundary condition in Martensen's method.

The reader may feel that the Dirichlet boundary condition stated might be insufficient to ensure flow parallel to the body surface and that the Neumann boundary condition should be imposed either in addition or instead. To counter this view let us first assume that Dirichlet is inadequate and that consequently there is a leakage velocity  $v_n$  normal to the body at  $a$ , Fig. 1.4. However if there are no sources present inside the body contour the only possibility is that the streamline  $\psi_0$  will cross the body a second time at point  $b$ . If we now apply the circulation theorem around the contour  $abc$  just inside the surface vorticity sheet, then

$$\oint_{abc} \mathbf{v} \cdot d\mathbf{s} = \int_a^b v_n ds + \int_b^a v_{si} ds = 0$$

A                      B

assuming also that there is no vorticity contained within the body profile. Since zero  $v_{si}$  has been enforced by the Dirichlet boundary condition, term  $B$  and therefore term  $A$  are independently zero. Since  $v_n$  is unidirectional along the supposed streamline  $\psi_0$ , the only possibility is that it must also be zero throughout. The Dirichlet condition is thus totally adequate provided there are no vortex or source distributions within the body profile. The reader is referred to Martensen (1959) for a rigorous proof.

## **1.5 Vorticity convection and production in a shear layer**

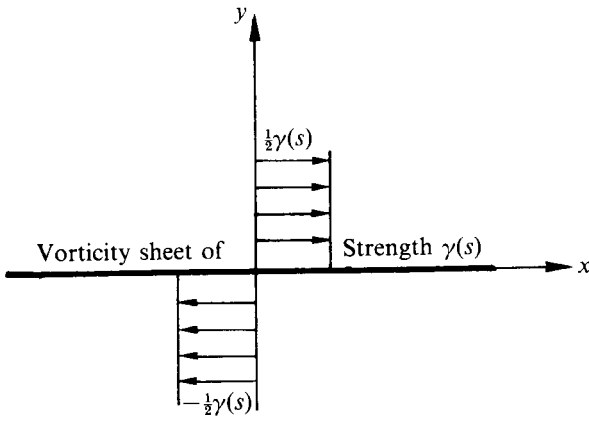
Most surface vorticity applications in the past have dealt with steady flows, for which the local surface vorticity  $\gamma(s)$  is constant with respect to time and is often regarded as bound to the surface. Thus in a two-dimensional steady flow situation the total bound circulation would be directly calculable through the contour integral

$$\Gamma = \oint \gamma(s) ds \quad (1.13)$$

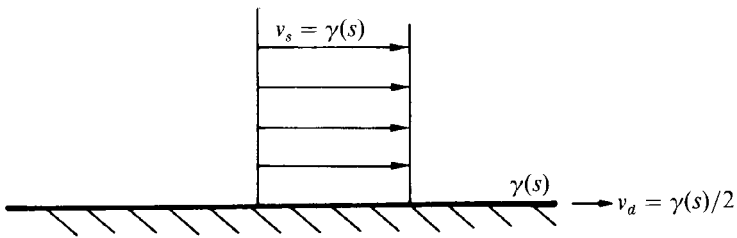
In reality however we know that the actual boundary layer vorticity is continuously being convected downstream, Fig. 1.3(c). Let us now consider the case of a vortex sheet of strength  $\gamma(s)$  coincident with the  $x$  axis and stretching between  $x = \pm\infty$ . Applying the circulation theorem again to an element  $\gamma(s) ds$  and taking into consideration symmetry about the  $x$  axis, Fig. 1.5(a), we see that the velocity above and below the sheet are given respectively by  $\pm\frac{1}{2}\gamma(s)$ . If we now superimpose a uniform stream of strength  $\frac{1}{2}\gamma(s)$  over the whole  $(x, y)$  plane we have a correct surface vorticity model for flow past a plane wall, Fig. 1.5(b). From this simple study we observe that for such a flow the vortex sheet, like the boundary layer which it represents, is also convected downstream, in this case with a velocity exactly equal to half of its strength,  $\frac{1}{2}\gamma(s)$ .

The foregoing argument was based upon the special case of flow past a plane wall, for which the surface vorticity is identical for all points on the wall. In fact the same principle applies to potential flow past bodies of arbitrary shape. Locally at point  $s$  the velocity changes from zero on the surface just beneath the vortex sheet, to the sheet convection velocity  $v_a = \frac{1}{2}\gamma(s)$  at the centre of the vorticity sheet, to  $v_s = \gamma(s)$  just outside the sheet. In this case of course  $\gamma(s)$  varies in magnitude along the wall, a fact which at first sight seems to be at odds with Kelvin's theorem of the constancy of circulation. Thus if the vorticity at  $s_2$  has been convected from  $s_1$  somewhere upstream, how is it possible that  $\gamma(s_2)$  does not equal  $\gamma(s_1)$  bearing in mind Kelvin's theorem? The simple answer to this seeming dilemma is that vorticity is continually being created or destroyed at a body surface in an inviscid flow whether the motion is steady or unsteady. Thus if we define  $d\gamma(s)$  as the net vorticity per unit length generated at point  $s$  in time  $dt$ , Fig. 1.3(b), then the net vorticity flux leaving the control volume  $abcd$  can be related to

*Vorticity convection and production in a shear layer*



(a) Vorticity sheet alone



(b) Vorticity sheet  $\gamma(s)$  with uniform stream  $\frac{1}{2}\gamma(s)$

Fig. 1.5. Surface vorticity model of a uniform stream past a plane wall.

$d\gamma(s)$  through

$$\text{Vorticity created in time } \Delta t = \frac{\text{Net vorticity flux, crossing } abcd}{\text{crossing } abcd}$$

that is

$$d\gamma(s) \cdot ds = \left\{ \frac{1}{2}(v_s + dv_s)(\gamma(s) + d\gamma(s)) - \frac{1}{2}v_s\gamma(s) \right\} dt$$

Neglecting second-order products of infinitesimal quantities and introducing (1.12) we have finally

$$\frac{d\gamma(s)}{dt} = \frac{d}{ds} \left( \frac{v_s^2}{2} \right) = -\frac{1}{\rho} \frac{dp}{ds} \tag{1.14}$$

This equation reveals the influence of the surface pressure gradient upon vorticity production in a potential flow. Surface vorticity is spontaneously generated if the pressure falls and is